Published in final edited form as:
Neurobiol Aging. 2015 February ; 36(2): 608–617. doi:10.1016/j.neurobiolaging.2014.10.030.

Fibrin deposited in the Alzheimer's disease brain promotes neuronal degeneration

Marta Cortes-Canteli, **Larissa Mattei**, **Allison T. Richards**, **Erin H. Norris**, and **Sidney Strickland**
Laboratory of Neurobiology and Genetics. The Rockefeller University. New York, USA

Abstract

Alzheimer's disease (AD) is the most common form of dementia and has no effective treatment. Besides the well-known pathological characteristics, this disease also has a vascular component, and substantial evidence shows increased thrombosis as well as a critical role for fibrin(ogen) in AD. This molecule has been implicated in neuroinflammation, neurovascular damage, blood brain barrier permeability, vascular amyloid deposition, and memory deficits that are observed in AD. Here we present evidence demonstrating that fibrin deposition increases in the AD brain and correlates with the degree of pathology. Moreover, we show that fibrin(ogen) is present in areas of dystrophic neurites and that a modest decrease in fibrinogen levels improves neuronal health and ameliorates amyloid pathology in the subiculum of AD mice. Our results further characterize the important role of fibrin(ogen) in this disease and support the design of therapeutic strategies aimed at blocking the interaction between fibrinogen and Aβ and/or normalizing the increased thrombosis present in AD.

Keywords

Fibrinogen; Alzheimer's disease; coagulation; neurodegeneration

1. Introduction

Alzheimer's disease (AD) is a multifactorial and severe neurodegenerative disorder for which there is no effective treatment available (Huang and Mucke, 2012). The 2009 World Alzheimer Report estimated that 35.6 million people worldwide were affected by dementia in 2010 and predicted more than 100 million people by 2050 (Prince and Jackson, 2009). Therefore, new therapeutic approaches are sorely needed. This disorder has brain pathological hallmarks such as amyloid-β (Aβ) plaques and neurofibrillary tangles (Selkoe,

Address correspondence to: Sidney Strickland. The Rockefeller University. 1230 York Avenue, New York, NY-10065, USA. Phone: (+1) 212-327-8705; Fax: (+1) 212-327-8774, strickland@rockefeller.edu.

Disclosure Statement
Authors declare no conflict of interest

2011) and is characterized by a progressive reduction in cortical thickness and an overall decrease in brain volume with a loss of neurons (Duyckaerts et al., 2009; Gomez-Isla et al., 1996) and synapses (Terry et al., 1991). Besides the strong correlation with different vascular risk factors such as atherosclerosis, hypertension, hypercholesterolemia, and diabetes (de la Torre, 2002; Humpel, 2011), AD pathogenesis also involves cerebrovascular abnormalities such as alterations to the neurovascular unit (Iadecola, 2010) and decreases in cerebral blood flow (Austin et al., 2011; Mazza et al., 2011), suggesting that vascular disease influences AD pathogenesis (Kalaria et al., 2012).

Fibrinogen is a plasma glycoprotein that circulates at high concentration in the blood and is essential for coagulation as it is converted into fibrin in response to injury (Weisel, 2005). The balance between clot formation and degradation needs to be tightly regulated since alterations in this system can induce and exacerbate pathological situations. Substantial evidence indicates a key role for fibrinogen and fibrin clot formation in AD pathogenesis. Increased fibrin(ogen) deposition is present in the brain parenchyma and in brain vessels of human AD patients (Cortes-Canteli et al., 2010; Cortes-Canteli et al., 2012; Cullen et al., 2005; Fiala et al., 2002; Lipinski and Sajdel-Sulkowska, 2006; Ryu and McLarnon, 2009; Viggars et al., 2011) and mouse models of AD (Cortes-Canteli et al., 2010; Paul et al., 2007). However, most of these studies involved the immunohistochemical analysis of fibrin(ogen) in the AD brain using antibodies that fail to distinguish fibrinogen and fibrin (hence the use of the term fibrin(ogen)), making it impossible to know whether the deposits are composed of one or the other, or a mixture of the two. Fibrin(ogen) co-localizes with Aβ in the AD brain (Cortes-Canteli et al., 2010; Cortes-Canteli et al., 2012; Jantaratnotai et al., 2010; Paul et al., 2007; Ryu and McLarnon, 2009), strongly interacts with this peptide (Ahn et al., 2010), and makes fibrin clots more difficult to degrade (Cortes-Canteli et al., 2010; Zamolodchikov and Strickland, 2012). AD mice are at high risk of arterial thrombosis (Jarre et al., 2014) and evidence indicates that there is increased obstruction of the cerebral blood vessels in the AD brain, which could strongly affect overall cerebral circulation. For example, aged ArcAβ AD mice have increased occlusion of functional intracortical microvessels (Klohs et al., 2012). Similarly, TgCRND8 AD mice show evidence of increased clotting in their brains and these fibrin clots are resistant to fibrinolysis (Cortes-Canteli et al., 2010). A prothrombotic state in AD patients is evidenced not only by increased clot formation, but also by decreased fibrinolysis and elevated levels of activated coagulation factors and platelets (Cortes-Canteli et al., 2012). Indeed, reducing fibrinogen levels has beneficial effects in AD mice such as decreasing blood brain barrier permeability (Paul et al., 2007; Ryu and McLarnon, 2009), neurovascular damage (Paul et al., 2007), inflammation (Paul et al., 2007; Ryu and McLarnon, 2009), and cerebral amyloid angiopathy (Cortes-Canteli et al., 2010). This enhancement in vascular function likely improves cerebral blood flow and hence neuronal function and survival, leading to the amelioration of memory deficits observed in AD mice after fibrinogen reduction (Cortes-Canteli et al., 2010). However, no studies have shown direct evidence that the levels of fibrin(ogen) have an effect on neuronal viability and function. Here, we demonstrate that fibrin(ogen) is present in areas packed with dystrophic neurites and plays a key role in neuronal viability, since decreasing fibrinogen levels reduces the amount of neuronal loss, synaptic dysfunction, and amyloid pathology present in AD mice. We also report that

insoluble fibrin accumulates in human and mouse AD brains and correlates with the degree of pathology. These results further characterize the role of fibrin(ogen) in AD pathophysiology and support the design of therapeutic strategies aimed at normalizing the irregular clotting observed in AD.

2. Methods

2.1 Mice

TgCRND8 mice express a double mutant form of the amyloid precursor protein 695 (KM670/671NL + V717F) (Chishti et al., 2001). These mice are on a mixed background (C57xCH3/C57) and develop age-dependent Aβ-pathology and memory deficits (provided by Drs. M.A. Chishti and D. Westaway, University of Toronto, Canada). Four-, 15-, 58- and 82-week-old TgCRND8 mice and their wild type littermates (n=3–7 mice/group) were thoroughly perfused with saline-heparin. Brains were removed, and one hemisphere was embedded, frozen in OCT, and processed for triple immunofluorescence analysis, while the cortex and hippocampus of the other hemisphere were dissected out and frozen for subsequent fibrin extraction.

Mice heterozygous for the *fibrinogen Aα chain* ($fbg^{+/-}$) (Suh et al., 1995) were crossed with TgCRND8 mice. TgCRND8; $fbg^{+/-}$ mice and their littermate controls were thoroughly perfused with saline-heparin, and brains were fixed in 4% paraformaldehyde, cryoprotected in 30% sucrose, frozen, and processed for NeuN, LAMP-1, and Congo Red determination.

All mice were genotyped twice, at time of weaning and at sacrifice. Mice were housed at The Rockefeller University's Comparative Biosciences Center and treated in accordance with IACUC-approved protocols.

2.2 Human samples

Human postmortem tissue was obtained from the Harvard Brain Tissue Resource Center. Blocks of frozen tissue from the superior frontal cortex (n=4 control and 15 AD cases), the anterior hippocampus with entorhinal cortex (n=4 control and 16 AD cases), and the hippocampal formation with parahippocampal gyrus (n=8 control and 29 AD cases) were sliced by cryostat (10 μm sections) for subsequent immunohistochemical analysis. Several sections were also collected in an Eppendorf tube for subsequent fibrin determination.

2.3 Fibrin extraction and Western blot

Mouse and human frozen tissue was homogenized in 5 volumes (g:ml) of phosphate buffered saline (PBS) containing 1% Nonidet P-40, 0.5% sodium deoxycholate, 0.1% SDS, and protease inhibitor cocktail (Roche). The homogenate was centrifuged at 4 °C at 10,000 g for 10 minutes, and the supernatant (soluble fraction) was transferred to a different tube. After several rounds of extraction, the insoluble (fibrin-containing) fraction was extracted as in (Tabrizi et al., 1999) with slight modifications. Briefly, the pellet was homogenized in 3 M urea, vortexed for 2 hours at 37 °C, and centrifuged at 14,000 g for 15 minutes. The supernatant was collected in a different tube, and the pellet was resuspended and vortexed at 65 °C for 30 minutes in reducing SDS loading buffer. Equal amounts were run on a 4–20%

gradient polyacrylamide Criterion gel (Bio-Rad), transferred to a polyvinylidene fluoride membrane (Pall), and incubated with the following antibodies: rabbit polyclonal anti-fibrin(ogen) antibody (gift from Dr. J. L. Degen, Cincinnati, Ohio, USA), mouse monoclonal anti-fibrin antibody (59D8 (Hui et al., 1983), gift from Dr. T. Renne, Karolinska Institutet, Sweden), mouse monoclonal anti-Aβ antibody (6E10, Covance), and rat monoclonal anti-tubulin antibody (YOL1/34, Abcam). Tubulin was used as loading control since it is present in different fractions after sequential solubilization steps and extensive rounds of extraction in the rat brain (Schindler et al., 2006). *In vitro* human or mouse fibrin clots were prepared as positive controls (Cortes-Canteli et al., 2010; Zamolodchikov and Strickland, 2012) and run in parallel with the samples. Samples were subjected to Western blot analysis 4–5 different times. Fibrin-β-chain and tubulin bands were quantified using NIH Image J software, and the ratio of fibrin:tubulin was plotted on a graph.

2.4 Human brain staining

Frozen human AD and control brain sections (10 μm) were fixed in 4% paraformaldehyde and treated with proteinase K (Dako) before performing the following staining protocols:

Fibrin immunohistochemistry- Sections were immersed in methanol/H_2O_2 to inactivate endogenous peroxidases, blocked in Tris buffer with 2% donkey:horse serum (1:1), and incubated overnight with the mouse monoclonal antibody 59D8 that specifically detects human fibrin (Hui et al., 1983). The following morning, sections were incubated with a biotinylated horse anti-mouse antibody, amplified by the VECTASTAIN Elite ABC Ready-to-Use Reagent, and developed using ImmPACT DAB Peroxidase Substrate (all from Vector Labs). Sections were then dehydrated, mounted, and imaged using a Zeiss Axiovert 200 microscope.

Triple immunofluorescence- Sections were blocked in Tris buffer with 2% goat serum followed by overnight incubation with a mouse monoclonal anti-human LAMP-1 antibody (clone H4A3, Developmental Studies Hybridoma Bank) and a rabbit polyclonal anti-human fibrinogen antibody (Dako). Then, the sections were incubated for 1 hour at RT with the highly cross-adsorbed secondary fluorescent antibodies CF405M goat anti-rabbit and CF555 goat anti-mouse (Biotium), rinsed, and incubated overnight with anti-Aβ monoclonal antibody 6E10 labeled with Alexa Fluor 488 (Covance). The tissue was incubated with 0.3 % Sudan Black B in 70% ethanol to block lipofuscin autofluorescence and finally covered with Vectashield (Vector Labs). Secondary controls omitting primary antibodies as well as controls using each individual primary antibody alone were carried out in parallel. An inverted TCS SP8 laser scanning confocal microscope (Leica) equipped with a fully tunable white light laser, a 405 nm laser, three HyD detectors and a HCX PL APO CS 40.0×1.10 water objective, available at The Rockefeller University Bio-Imaging Resource Center, was used to acquire the images. Sixteen bit images of areas rich in amyloid were taken sequentially at 1024×1024, at 600 Hz scan speed and keeping laser and exposure conditions constant in all 3 channels. An average of 3–4 pictures per section was taken, and the percentage of co-localization between the different markers was analyzed using MetaMorph software (Molecular Devices). The region of interest, comprised of Aβ staining, was marked, and then images were separated into the 3 channels (blue, green, and red),

thresholded, and transformed to binary. The total number of pixels in each of these original binary images was recorded. Images were then combined using "logical *AND*", first in pairs (blue-green, blue-red, and green-blue) and then in a trio (blue-green-red). The resulting binary images show only those pixels positive in the combined channels and therefore the percentage of co- and tri-localization was calculated by comparing these with the total number of pixels in each of the original binary images.

2.5 Mouse brain staining

Triple immunofluorescence - Frozen coronal sections (20 μm) from 4-, 15-, 58-, and 82-week-old TgCRND8 mice and their wild type littermates (n=3–8 mice/group) were fixed in cold ethanol and treated for 2 minutes with Proteinase K (Dako) diluted 1:4 in Tris buffer. Fibrin(ogen) immunohistochemistry was performed using a rabbit polyclonal biotinylated anti-fibrin(ogen) antibody (Abcam) and the Tyramide Signal Amplification system (Perkin Elmer), according to manufacturer's instructions. A control using biotinylated rabbit IgG in place of anti-fibrin(ogen) antibody was included to verify the specificity of the antibody. Fibrin(ogen) was visualized using CF405M streptavidin (Biotium). Sections then were blocked for 1 hour in PBS containing 0.25% Triton X-100 and 3% goat serum (Vector Labs) and incubated overnight at 4 °C with rat monoclonal anti-mouse LAMP-1 antibody (clone 1D4B, Developmental Studies Hybridoma Bank) and 6E10 Alexa Fluor 488-conjugated anti-Aβ mouse monoclonal antibody (Covance). Sections were then incubated for 2 hours with Alexa Fluor 594 goat anti-rat secondary antibody, and cover-slipped with Vectashield (Vector Labs). Secondary controls omitting primary antibodies as well as controls using each individual primary antibody alone were carried out in parallel. Images from the cortex and hippocampus were taken and quantified as described above for the triple immunofluorescence performed in human sections.

NeuN immunohistochemistry and quantification- Floating coronal sections (20 μm) from 82-week-old TgCRND8;*fbg*$^{+/+}$mice, TgCRND8;*fbg*$^{+/-}$ mice, and their wild type littermate controls (n= 3–7 mice/group) were processed for immunohistochemistry using a mouse monoclonal NeuN antibody (Chemicon) to identify neurons. The Vector Mouse-on-Mouse kit (Vector Labs) was used according to the manufacturer's instructions to decrease non-specific staining due to endogenous immunoglobulins. The diaminobenzidine method was used for development. Counterstaining with 0.5% Thioflavin S (Sigma) was performed to identify amyloid (not shown). Low magnification images were captured to identify the corresponding Bregma of each section analyzed. High magnification images of the entire dorsal subiculum area were taken using a 20x objective to avoid oversampling errors. The dorsal subiculum is adjacent to the CA1 layer and expands from Bregma −2.54 mm to −3.80 mm (Franklin and Paxinos, 2008). Since its shape, size, and structure change substantially along its anatomy, we focused our study on the central region of the dorsal subiculum. NeuN-positive cells were quantified in every ~ 4th coronal section covering the unilateral dorsal subiculum from Bregma −2.7 mm to −3.4 mm. The total number of NeuN-positive cells and the area analyzed were measured in each section using Image J. A total of 160 sections (~8 sections/mouse) were analyzed, averaged per group, and plotted relative to the wild type control. To avoid differences in neuronal density among the different Bregmas, the average of analyzed sections per mouse and per group was maintained at Bregma −3.0 mm.

Lamp-1 and Congo Red staining and quantification- Floating coronal sections (20 μm) from 82-week-old TgCRND8;*fbg*$^{+/+}$ and TgCRND8;*fbg*$^{+/-}$ mice were washed in PBS, blocked for 1 hour in PBS containing 0.25% Triton X-100 and 3% goat serum (Vector Labs), and incubated overnight at 4 °C with rat monoclonal anti-mouse LAMP-1 antibody (clone 1D4B, Developmental Studies Hybridoma Bank) and mouse monoclonal anti-NeuN antibody. Sections were then incubated for 2 hours with Alexa Fluor 488 goat anti-rat and Alexa Fluor 647 goat anti-mouse secondary antibodies (Invitrogen), mounted, and counterstained with 0.2% Congo Red (Sigma) dissolved in 70% isopropanol. Sections were cover-slipped with Vectashield and imaged using an inverted Leica TCS SP5 laser scanning confocal microscope equipped with a fully tunable white light laser, two HyD detectors, one PMT detector, and a super-Z stage for rapid tiling, available at The Rockefeller University Bio-Imaging Resource Center. Z-stack tile-scans covering the subicular area (identified by NeuN staining) were acquired in all three channels using a HCX PL APO CS 40.0×1.10 water objective. Twelve bit images were taken at 1024×1024, at 600 Hz scan speed. Laser and exposure conditions were kept constant between genotypes. Reconstructed tile scan images were thresholded in Image J, and the LAMP-1- and Congo Red-positive areas were quantified in each individual plane. The total LAMP-1- and Congo Red-positive areas in the subiculum were then calculated in each section, averaged, and compared between groups.

2.6 Statistics

All numerical values are presented as mean ± SEM. Statistical analysis in human samples was performed using the non-parametric Mann-Whitney test. Statistical significance in mouse samples was determined using two-tailed t test analysis comparing the different experimental groups. Two-way ANOVA and Bonferroni post-test were also performed to determine whether the effect of genotype and treatment were considered significant. *P* values below 0.05 were considered significant.

3. Results

3.1 Fibrin is present in the AD brain and correlates with the degree of pathology

Fibrin(ogen) is abnormally deposited in the AD brain. It is important to know whether these deposits are composed of fibrinogen, fibrin, or a mixture of the two. It is also critical to understand whether fibrin(ogen) accumulation correlates with the degree of AD pathology and to quantify the actual level of fibrin(ogen) deposition compared to controls. To that end, we extracted the insoluble protein fraction, where fibrin is located (Tabrizi et al., 1999), from different regions of human postmortem brain samples and compared non-demented controls with AD patients. As shown in top panels of Figure 1A–C, fibrin is present in the brains of human AD patients. The main product detected, fibrin-β chain at ~52 kDa, is significantly increased in AD samples in all the areas of the brain analyzed compared to non-demented control samples (Figure 1D–F). As expected, control patients present with very low amounts of insoluble fibrin in the brain. We detected more than a 100-fold increase in fibrin deposition in the superior frontal cortex (Figure 1D, 0.12±0.05 control *vs* 13.45±11.6 AD; *p<0.05), a 23-fold increase in the anterior hippocampus (Figure 1E, 0.04±0.01 control *vs* 0.99±0.3 AD; **p<0.01), and more than a 20-fold increase in the hippocampus (Figure 1F, 0.06±0.01 control *vs* 1.3±0.3 AD; ***p<0.001) of AD patients

compared to non-demented controls. We re-probed the membrane with a specific monoclonal antibody against human fibrin, clone 59D8 (Hui et al., 1983), and obtained similar results (Figure 1A–C, middle panels), confirming that the majority of the soluble fibrinogen was indeed removed during the extraction protocol and we are detecting mostly insoluble fibrin. The membranes were re-probed with a tubulin antibody as loading control (Figure 1A–C, bottom panels). The intermediate fractions generated during this extraction protocol (the soluble and urea supernatant fractions) were also analyzed (data not shown). No fibrin was detected in any of those fractions, confirming that fibrin was not lost in any steps of the protocol and that all the fibrin deposited in the brain was being detected.

We next analyzed the localization of fibrin in the set of AD patients that presented with high levels of this protein deposited in the hippocampus (Figure 1C). Immunohistochemical analysis revealed different patterns of fibrin distribution. Some of the AD patients analyzed presented fibrin exclusively within the vasculature, lining big vessels (Figure 1G), blocking capillaries (Figure 1H and I), or a combination of both (Figure 1J). Other AD patients showed fibrin extravasated as perivascular leakage “clouds” (Figure 1K and L) or into the brain parenchyma (Figure 1M and N).

In order to analyze the amount of fibrin in a more uniform system, we used AD mice. While AD mouse models do not fully recapitulate the human disease, they are more homogeneous than humans and allow for a better in-depth analysis of specific components since they accumulate Aβ and develop pathology as they age. We examined the amount of fibrin present in the cortex and hippocampus of TgCRND8 AD mice (Chishti et al., 2001) at 4, 15, 58, and 82 weeks (Figure 2), ages that correspond to different stages of AD pathology (Chishti et al., 2001). As previously described for human brain tissue, we extracted and analyzed the insoluble fractions by Western blot. We observed low amounts of fibrin-β chain in the brains of 4-week-old mice, when no Aβ pathology was present. However, the amount of fibrin significantly increased in the brains of 58- and 82-week-old AD mice compared to their age-matched wild type littermates (Figure 2A, upper panels, and B). Moreover, this significant increase in fibrin appeared to correlate with Aβ pathology, as detected by the 6E10 antibody (Figure 2, middle panels). The membranes were reprobed with a tubulin antibody as loading control (Figure 2, bottom panels). Unfortunately, the human-specific fibrin antibody 59D8 recognized mouse fibrin very weakly in the positive control (data not shown) and therefore could not be used to properly detect fibrin in these specimens. In order to identify where this fibrin deposition was taking place, we performed immunostaining in the same set of TgCRND8 mice. Double immunofluorescence showed that fibrin(ogen) and Aβ increase with age in the AD brain, reproducing the results obtained in Figure 2A, and that fibrin(ogen) deposits co-localize with Aβ in amyloid plaques (Figure 2C).

Overall, these results demonstrated that fibrin, the main protein component of blood clots, accumulates in the human and mouse AD brain where it appears to correlate with the degree of Aβ pathology.

3.2 Fibrin(ogen) is present in areas of dystrophic neurites and amyloid pathology in the AD brain

We investigated whether fibrin(ogen) is present in areas of synaptic dysfunction, one of the first and most important pathological hallmarks of AD that correlates very well with cognitive decline (Terry et al., 1991). Since lysosomes and other autophagy-related organelles are part of the neuritic dystrophy observed in AD (Lee et al., 2011; Nixon et al., 2005), we stained for the lysosomal-associated membrane protein-1 (LAMP-1) to identify areas of synaptic dysfunction. This marker is highly up-regulated in the human AD brain (Barrachina et al., 2006) and cerebrospinal fluid (Armstrong et al., 2014), as well as highly enriched in the dystrophic areas surrounding amyloid plaques in AD mice (Condello et al., 2011; Hashimoto et al., 2010) and human AD patient brains (Barrachina et al., 2006; Perez-Gracia et al., 2008). Human postmortem hippocampal sections were co-stained for fibrin(ogen), LAMP-1, and Aβ (Figure 3A). Fibrin(ogen) was present in areas of dystrophic neurites along with Aβ deposition. Several patterns of fibrin(ogen) deposition were found in the different AD patients: Fibrin(ogen) was present in the core of fibrillar plaques (arrows in AD Patient 1, Figure 3A), diffuse amyloid (arrowheads in AD Patient 1, Figure 3A) and was also found co-localized with Aβ staining and areas of synaptic dysfunction in the vicinity of blood vessels (arrow in AD Patient 2, Figure 3A). Confocal analysis and subsequent quantification revealed that 16.7% (± 4.1) of the fibrin(ogen) staining present in amyloid areas in the human AD brain was co-localized with Aβ, and 37.1% (±4.6) with LAMP-1. The amount of fibrin(ogen) co-localized with both markers had an average of 9.7% (± 2.2) overlap of pixels from all three molecules, with a maximum in some areas of 49.9% tri-localization. Nevertheless, it should be emphasized that the three markers do not need to be fully overlapping to impact each other's function and play a role in AD pathophysiology. For example, fibrin(ogen) is a strong pro-inflammatory molecule (Davalos and Akassoglou, 2012), and therefore its presence in abnormal deposits in or around amyloid plaques could exacerbate the inflammatory response already present in AD and promote neuronal dysfunction (Solito and Sastre, 2012). In order to do this, fibrin(ogen) does not need to be co-localized with these markers but rather be in the same area.

We next investigated whether the abnormal accumulation of fibrin(ogen) present in the AD mouse brain (Figure 2) coincided with areas of synaptic dysfunction. Triple immunofluorescence analysis showed that fibrin(ogen) accumulated in areas rich in LAMP-1 as well as Aβ staining in the brains of 82-week-old TgCRND8 AD mice (Figure 3B). The accumulation pattern was more homogeneous than what was found in the human AD brain, with most of the fibrin(ogen) observed in patches that often coincided with areas of dystrophic neurites as well as Aβ pathology (arrows in Figure 3B). Quantification analysis showed that 29.6% (±6.2) of fibrin(ogen) staining present in amyloid areas co-localized with Aβ and 36.1% (± 5.8) with LAMP-1. The percentage of pixels with tri-localization had an average of 13.3% (± 2.7), with a maximum in some areas of 53.8% tri-localization.

These results provide further evidence that fibrin(ogen) is not only abnormally present in the AD brain co-localizing with Aβ, but is also found in areas fully packed with dystrophic neurites.

3.3 Decreasing fibrinogen levels reduces neuronal death in the dorsal subiculum of AD mice

Since significant amounts of fibrin are found in the AD mouse brain (Figure 2) and fibrin(ogen) is present in areas of synaptic dysfunction and Aβ pathology (Figure 3), we investigated whether modulating fibrinogen levels could affect the characteristic loss of neurons present in AD. Although most of the AD mouse models do not present robust and widespread neuronal death as the human AD brain does (Duyckaerts et al., 2008; Gomez-Isla et al., 1996), localized neurodegeneration has been reported in some AD mouse lines (Wirths and Bayer, 2010) in areas such as the subiculum (Oakley et al., 2006). The subiculum is a relatively well-defined structure of the hippocampus that plays an essential role in memory processing (O'Mara, 2005) and is profoundly affected in AD (Falke et al., 2003). Immunohistochemical analysis using the specific neuronal marker NeuN showed a dramatic reduction in the number of neurons present in the dorsal subiculum of 82-week-old TgCRND8 AD mice (Figure 4, A *vs* C). We quantified the extent of neuronal loss in this area, revealing that 82-week-old TgCRND8 mice have ~25% fewer subicular neurons than their wild type littermates (Figure 4E). This result is in line with stereological studies performed on the human AD hippocampus (Zilkova et al., 2006).

We then determined whether reducing fibrinogen levels could affect neuronal health in TgCRND8 mice. We used TgCRND8 mice heterozygous for a mutation in the *fibrinogen Aα chain* gene, TgCRND8; $fbg^{+/-}$ mice, that have a ~30% decrease in fibrinogen levels (Suh et al., 1995). We focused our studies on 82-week-old TgCRND8; $fbg^{+/-}$ mice since fibrin levels peaked at that age (Figure 2). NeuN immunohistochemistry and subsequent quantification showed that AD mice with only one copy of the *fibrinogen* gene had significantly more neurons in the dorsal subiculum than AD littermate controls (Figure 4, C *vs* D; E; 73.3% ± 1.7 TgCRND8; $fbg^{+/+}$ mice *vs* 78.2% ± 1.3 TgCRND8; $fbg^{+/-}$ mice; *$p<0.05$). Bearing one copy of the *fibrinogen* gene did not affect the overall amount of neurons in the subiculum of wild type littermates (Figure 4, A *vs* B; E). These results indicate that fibrinogen levels affect the neuronal loss observed in the AD mouse brain.

3.4 Decreasing fibrinogen levels ameliorates synaptic dysfunction and amyloid pathology in the subiculum of AD mice

Since neuronal loss is accompanied by a reduction in synapses, we investigated if reducing fibrinogen levels could ameliorate the degree of synaptic dysfunction in the AD brain. As in Figure 3, we used LAMP-1 as a marker of dystrophic neurites since it provides an excellent contrast with the surrounding tissue (Condello et al., 2011) and thus allows for quantification of the dystrophic area. In addition to LAMP-1, we co-stained brain sections with anti-NeuN antibody to identify the dorsal subiculum and with Congo Red to detect amyloid plaques. We acquired high resolution confocal Z-stack tile-scans covering the subicular area in all 3 channels (Figure 5, A–F). The total LAMP-1-positive area was quantified within the subiculum and compared between 82-week-old TgCRND8; $fbg^{+/+}$ mice and TgCRND8; $fbg^{+/-}$ mice. We found a 25% decrease in the amount of dystrophic neurites in the dorsal subiculum of AD mice with just one copy of the *fibrinogen* gene (Figure 5G; 100% ± 10.7 TgCRND8; $fbg^{+/+}$ mice *vs* 74.5% ± 7 TgCRND8; $fbg^{+/-}$ mice; *$p<0.05$). We also observed that reducing fibrinogen levels provoked a marked reduction in

the amount of amyloid pathology present in that area (Figure 5H; 100% ± 11.6 TgCRND8; *fbg*$^{+/+}$ mice *vs* 58.2% ± 5.9 TgCRND8; *fbg*$^{+/-}$ mice; **p<0.01). These results indicate that fibrin(ogen) plays a role in synaptic degeneration as well as Aβ accumulation in the AD brain.

4. Discussion

AD is a multifactorial disease with a vascular component, and increasing evidence suggests that fibrinogen and fibrin clot formation contribute to this disorder. Here we further investigated the role of this plasma protein in AD pathogenesis using human postmortem AD samples and AD mice. High levels of fibrin were found in the brains of AD patients and AD mice, and these levels appeared to correlate with the degree of Aβ pathology. We also observed that fibrin(ogen) was present in areas where neurons were degenerating and losing their synapses, affecting neuronal health. These findings advance our understanding of fibrin(ogen)'s contribution to the pathophysiology of AD.

In order to find a therapeutic strategy aimed at normalizing the increased thrombosis present in AD, it is critical to know which are the key players as well as their localization and partners. We found that the insoluble fibrin polymer, the end point of the coagulation cascade, is abnormally present in different areas of the human AD brain intra- and extra-vascularly (Figure 1), as well as in the brains of AD mice where it increases over time and correlates with the level of Aβ deposition (Figure 2). Having large vessels lined with fibrin or capillaries completely blocked by its deposition (Figure 1G–J) can alter the cerebral blood flow, especially if these vascular occlusions occur chronically over the course of many years. This could play a substantial role on the hypoperfusion present in AD patients (Austin et al., 2011; Mazza et al., 2011). Also, extravascular fibrin deposition (Figure 1K–N) could exacerbate the chronic inflammation present in the AD brain, recruit different cells types, and promote processes such as extracellular matrix binding as well as platelet and endothelial cell spreading (Mosesson, 2005). All of these events could have a deleterious effect on the brain's balanced activity.

We noticed the distribution as well as the amount of fibrin present in the brain was variable within AD patients. The AD population is very heterogeneous since different pathways are affected in this disease, which could explain why we identified only a subpopulation of AD patients with increased thrombosis. We believe this variability reinforces the fact that this disease is multifactorial and stresses the importance of developing individualized diagnosis and treatment depending on the different pathologies present in each specific AD patient.

Altered expression of postsynaptic (Gylys et al., 2004) as well as presynaptic proteins (Masliah et al., 1994) occurs in human AD patients as well as in AD mouse lines (Oakley et al., 2006). Neurodegeneration is also an important pathological component of AD as loss of neurons occurs in multiples areas of the human AD brain (Duyckaerts et al., 2009). We report that fibrin(ogen) is present in areas packed with dystrophic neurites (Figure 3), and more importantly, reducing fibrinogen levels increased the amount of subicular neurons by 5% (Figure 4), decreased synaptic dysfunction by 25% (Figure 5), and reduced amyloid pathology by more than 40% (Figure 5). These results strongly suggest that the presence of

fibrin(ogen) might be neurotoxic in this region. However, it is possible that decreasing fibrinogen levels also affects the balance of other blood- or vessel-derived proteins known to be present in microhemorrhages close to amyloid plaques (Cullen et al., 2005; Cullen et al., 2006). Therefore, neuronal dysfunction near fibrin(ogen)-positive areas may be due to direct fibrin toxicity and/or may also be the result of a chronic vascular disease. It is possible that we did not see a bigger effect because the reduction in plasma fibrinogen levels in these mice is only ~30%, and fibrino(ogen) is certainly not the only factor affecting amyloid deposition and neuronal dysfunction in AD pathology. However, even the modest 5% increase in neurons we observed due to decreasing fibrinogen levels represents ~300 subicular neurons/mm^2, which together with the reduction in dystrophic neurites and amyloid pathology, could have a significant impact on AD progression. Since the AD brain atrophies at a rate of nearly 3% per year (Hua et al., 2013), identifying therapeutic strategies that can decrease that rate could delay disease progression considerably. Interventions with a modest interruption in disease onset and progression by one year could translate into avoiding 9 million AD cases by 2050 (Brookmeyer et al., 2007).

The present studies confirm the increased thrombosis present in the AD brain, which can profoundly affect brain physiology. Several factors in AD could be responsible for this increased thrombosis. Since there is an extensive cross-talk between inflammation and hemostasis (Levi et al., 2004), the widespread inflammatory response present in AD (Lee et al., 2010) may lead to a pro-coagulant state which in turn sustains inflammation. Indeed, increased thrombin generation as well as elevated levels of activated coagulation factors and activated platelets are present in the AD circulation and brain (Cortes-Canteli et al., 2012). In addition, episodes of microhemorrhages can occur in the AD brain (Cullen et al., 2005; Cullen et al., 2006), suggesting that blood-derived proteins, including fibrinogen, are able to cross the blood brain barrier over long periods of time and deposit in the AD brain. Due to this prothrombotic state, it is possible that when fibrinogen extravasates into the brain, it is converted into fibrin, where it might persist, since the fibrinolytic system is reduced in the AD brain (Ledesma et al., 2000; Melchor et al., 2003). Moreover, the presence of elevated Aβ in the brain would promote its binding to fibrin(ogen) (Ahn et al., 2010) and incorporate into fibrin clots, further delaying fibrinolysis (Cortes-Canteli et al., 2010; Zamolodchikov and Strickland, 2012). This fibrin deposition could then decrease cerebral blood flow, promote inflammation, and affect neuronal function, ultimately leading to cell death and cognitive deficits.

It remains to be clarified whether fibrin(ogen) deposition is a cause or a consequence of AD. High levels of fibrinogen in plasma increase the risk for dementia (van Oijen et al., 2005; Xu et al., 2008), and fibrinogen in cerebrospinal fluid (Craig-Schapiro et al., 2011; Vafadar-Isfahani et al., 2012) and plasma (Thambisetty et al., 2011; Yang et al., 2014) has been proposed as a useful biomarker to identify AD progression. Interestingly, fibrinogen has recently been found to be one of the few blood-based biomarkers specific for AD and not for other brain disorders (Chiam et al., 2014). However, whether fibrin(ogen) deposition and fibrin clot formation precedes or follows AD pathology is still an open question as is whether this disorder is caused by primary or secondary cerebral blood flow deficiency (Austin et al., 2011; Mazza et al., 2011). What is clear is that fibrinogen and fibrin clot formation contribute to AD pathogenesis by increasing neurovascular damage (Paul et al.,

2007), neuroinflammation (Paul et al., 2007), cerebral amyloid angiopathy (Cortes-Canteli et al., 2010), and neuronal degeneration (present study). Therefore, therapeutic strategies aimed at blocking the interaction between fibrinogen and Aβ (Ahn et al., 2014) or at normalizing thrombosis and decreasing the accumulation of fibrin(ogen) in the AD brain could prove useful in improving cerebral blood flow, neuronal function, and survival, which in turn could have significant long-term benefits for AD patients.

Acknowledgments

This work was supported by the BrightFocus Foundation, NIH grant NS050537, Litwin Foundation, May and Samuel Rudin Family Foundation, Blanchette Hooker Rockefeller Fund, Mellam Family Foundation, and John A. Herrmann, Jr. We thank Drs. M. Azhar Chishti and David Westaway (University of Toronto, Toronto, Canada) for providing the TgCRND8 mice and Dr. Jay L. Degen (Cincinnati, Ohio, USA) and Dr. T. Renne (Karolinska Institutet, Sweden) for providing the fibrin(ogen) and fibrin antibodies, respectively. We thank Strickland Lab members for thoughtful discussions, particularly Daria Zamolodchikov for her expert advice on the detection of fibrin by Western blot and Andrew Lawson for his hard work and discussions during his summer project. We also thank Jose Miguel Cortes and Shaine Abbani for technical help and The Rockefeller University's Bio-Imaging Resource Center members for their help and support. Human brain samples were provided by the Harvard Brain Tissue Resource Center, which is supported in part by PHS grant number R24 MH068855. Monoclonal LAMP-1 antibodies (1D4B and H4A3) developed by J. Thomas August and James E.K. Hildreth (Johns Hopkins University School of Medicine, Baltimore, MD) were obtained from the Developmental Studies Hybridoma Bank developed under auspices of the NICHD and maintained by The University of Iowa (Department of Biology, Iowa City, IA 52242).

References

Ahn HJ, Glickman JF, Poon KL, Zamolodchikov D, Jno-Charles OC, Norris EH, Strickland S. A novel Abeta-fibrinogen interaction inhibitor rescues altered thrombosis and cognitive decline in Alzheimer's disease mice. J Exp Med. 2014; 211:1049–1062. [PubMed: 24821909]

Ahn HJ, Zamolodchikov D, Cortes-Canteli M, Norris EH, Glickman JF, Strickland S. Alzheimer's disease peptide {beta}-amyloid interacts with fibrinogen and induces its oligomerization. Proc Natl Acad Sci U S A. 2010; 107:21812–21817. [PubMed: 21098282]

Armstrong A, Mattsson N, Appelqvist H, Janefjord C, Sandin L, Agholme L, Olsson B, Svensson S, Blennow K, Zetterberg H, et al. Lysosomal Network Proteins as Potential Novel CSF Biomarkers for Alzheimer's Disease. Neuromolecular Med. 2014; 16:150–160. [PubMed: 24101586]

Austin BP, Nair VA, Meier TB, Xu G, Rowley HA, Carlsson CM, Johnson SC, Prabhakaran V. Effects of hypoperfusion in Alzheimer's disease. J Alzheimers Dis. 2011; 26(Suppl 3):123–133. [PubMed: 21971457]

Barrachina M, Maes T, Buesa C, Ferrer I. Lysosome-associated membrane protein 1 (LAMP-1) in Alzheimer's disease. Neuropathol Appl Neurobiol. 2006; 32:505–516. [PubMed: 16972884]

Brookmeyer R, Johnson E, Ziegler-Graham K, Arrighi HM. Forecasting the global burden of Alzheimer's disease. Alzheimer's & Dementia. 2007; 3:186–191.

Chiam JTW, Dobson RJB, Kiddle SJ, Sattlecker M. Are Blood-Based Protein Biomarkers for Alzheimer's Disease also Involved in Other Brain Disorders? A Systematic Review. J Alzheimers Dis. 2014 Epub Ahead of Print.

Chishti MA, Yang DS, Janus C, Phinney AL, Horne P, Pearson J, Strome R, Zuker N, Loukides J, French J, et al. Early-onset amyloid deposition and cognitive deficits in transgenic mice expressing a double mutant form of amyloid precursor protein 695. J Biol Chem. 2001; 276:21562–21570. [PubMed: 11279122]

Condello C, Schain A, Grutzendler J. Multicolor time-stamp reveals the dynamics and toxicity of amyloid deposition. Scientific reports. 2011; 1:19. [PubMed: 22355538]

Cortes-Canteli M, Paul J, Norris EH, Bronstein R, Ahn HJ, Zamolodchikov D, Bhuvanendran S, Fenz KM, Strickland S. Fibrinogen and beta-amyloid association alters thrombosis and fibrinolysis: a possible contributing factor to Alzheimer's disease. Neuron. 2010; 66:695–709. [PubMed: 20547128]

Cortes-Canteli M, Zamolodchikov D, Ahn HJ, Strickland S, Norris EH. Fibrinogen and altered hemostasis in Alzheimer's disease. J Alzheimers Dis. 2012; 32:599–608. [PubMed: 22869464]

Craig-Schapiro R, Kuhn M, Xiong C, Pickering EH, Liu J, Misko TP, Perrin RJ, Bales KR, Soares H, Fagan AM, et al. Multiplexed immunoassay panel identifies novel CSF biomarkers for Alzheimer's disease diagnosis and prognosis. PloS one. 2011; 6:e18850. [PubMed: 21526197]

Cullen KM, Kocsi Z, Stone J. Pericapillary haem-rich deposits: evidence for microhaemorrhages in aging human cerebral cortex. J Cereb Blood Flow Metab. 2005; 25:1656–1667. [PubMed: 15917745]

Cullen KM, Kócsi Z, Stone J. Microvascular pathology in the aging human brain: Evidence that senile plaques are sites of microhaemorrhages. Neurobiol Aging. 2006; 27:1786–1796. [PubMed: 17063559]

Davalos D, Akassoglou K. Fibrinogen as a key regulator of inflammation in disease. Seminars in immunopathology. 2012; 34:43–62. [PubMed: 22037947]

de la Torre JC. Alzheimer disease as a vascular disorder: nosological evidence. Stroke. 2002; 33:1152–1162. [PubMed: 11935076]

Duyckaerts C, Delatour B, Potier MC. Classification and basic pathology of Alzheimer disease. Acta Neuropathol. 2009; 118:5–36. [PubMed: 19381658]

Duyckaerts C, Potier MC, Delatour B. Alzheimer disease models and human neuropathology: similarities and differences. Acta Neuropathol. 2008; 115:5–38. [PubMed: 18038275]

Falke E, Nissanov J, Mitchell TW, Bennett DA, Trojanowski JQ, Arnold SE. Subicular dendritic arborization in Alzheimer's disease correlates with neurofibrillary tangle density. Am J Pathol. 2003; 163:1615–1621. [PubMed: 14507668]

Fiala M, Liu QN, Sayre J, Pop V, Brahmandam V, Graves MC, Vinters HV. Cyclooxygenase-2-positive macrophages infiltrate the Alzheimer's disease brain and damage the blood-brain barrier. Eur J Clin Invest. 2002; 32:360–371. [PubMed: 12027877]

Franklin, KBJ.; Paxinos, G. The mouse brain in stereotaxic coordinates. 3. Amsterdam; London: Elsevier; 2008.

Gomez-Isla T, Price JL, McKeel DW Jr, Morris JC, Growdon JH, Hyman BT. Profound loss of layer II entorhinal cortex neurons occurs in very mild Alzheimer's disease. J Neurosci. 1996; 16:4491–4500. [PubMed: 8699259]

Gylys KH, Fein JA, Yang F, Wiley DJ, Miller CA, Cole GM. Synaptic changes in Alzheimer's disease: increased amyloid-beta and gliosis in surviving terminals is accompanied by decreased PSD-95 fluorescence. Am J Pathol. 2004; 165:1809–1817. [PubMed: 15509549]

Hashimoto T, Ogino K, Shin RW, Kitamoto T, Kikuchi T, Shimizu N. Age-dependent increase in lysosome-associated membrane protein 1 and early-onset behavioral deficits in APPSL transgenic mouse model of Alzheimer's disease. Neurosci Lett. 2010; 469:273–277. [PubMed: 20025930]

Hua X, Hibar DP, Ching CR, Boyle CP, Rajagopalan P, Gutman BA, Leow AD, Toga AW, Jack CR Jr, Harvey D, et al. Unbiased tensor-based morphometry: improved robustness and sample size estimates for Alzheimer's disease clinical trials. NeuroImage. 2013; 66:648–661. [PubMed: 23153970]

Huang Y, Mucke L. Alzheimer Mechanisms and Therapeutic Strategies. Cell. 2012; 148:1204–1222. [PubMed: 22424230]

Hui KY, Haber E, Matsueda GR. Monoclonal antibodies to a synthetic fibrin-like peptide bind to human fibrin but not fibrinogen. Science. 1983; 222:1129–1132. [PubMed: 6648524]

Humpel C. Chronic mild cerebrovascular dysfunction as a cause for Alzheimer's disease? Exp Gerontol. 2011; 46:225–232. [PubMed: 21112383]

Iadecola C. The overlap between neurodegenerative and vascular factors in the pathogenesis of dementia. Acta Neuropathol. 2010; 120:287–296. [PubMed: 20623294]

Jantaratnotai N, Schwab C, Ryu JK, McGeer PL, McLarnon JG. Converging perturbed microvasculature and microglial clusters characterize Alzheimer disease brain. Curr Alzheimer Res. 2010; 7:625–636. [PubMed: 20704556]

Jarre A, Gowert NS, Donner L, Münzer P, Klier M, Borst O, Schaller M, Lang F, Korth C, Elvers M. Pre-activated blood platelets and a pro-thrombotic phenotype in APP23 mice modeling Alzheimer's disease. Cell Signal. 2014; 26:2040–2050. [PubMed: 24928203]

Kalaria RN, Akinyemi R, Ihara M. Does vascular pathology contribute to Alzheimer changes? J Neurol Sci. 2012; 322:141–147. [PubMed: 22884479]

Klohs J, Baltes C, Princz-Kranz F, Ratering D, Nitsch RM, Knuesel I, Rudin M. Contrast-enhanced magnetic resonance microangiography reveals remodeling of the cerebral microvasculature in transgenic ArcAbeta mice. J Neurosci. 2012; 32:1705–1713. [PubMed: 22302811]

Ledesma MD, Da Silva JS, Crassaerts K, Delacourte A, De Strooper B, Dotti CG. Brain plasmin enhances APP alpha-cleavage and Abeta degradation and is reduced in Alzheimer's disease brains. EMBO Rep. 2000; 1:530–535. [PubMed: 11263499]

Lee S, Sato Y, Nixon RA. Lysosomal Proteolysis Inhibition Selectively Disrupts Axonal Transport of Degradative Organelles and Causes an Alzheimer's-Like Axonal Dystrophy. J Neurosci. 2011; 31:7817–7830. [PubMed: 21613495]

Lee YJ, Han SB, Nam SY, Oh KW, Hong JT. Inflammation and Alzheimer's disease. Arch Pharm Res. 2010; 33:1539–1556. [PubMed: 21052932]

Levi M, van der Poll T, Buller HR. Bidirectional relation between inflammation and coagulation. Circulation. 2004; 109:2698–2704. [PubMed: 15184294]

Lipinski B, Sajdel-Sulkowska EM. New insight into Alzheimer disease: demonstration of fibrin(ogen)-serum albumin insoluble deposits in brain tissue. Alzheimer Dis Assoc Disord. 2006; 20:323–326. [PubMed: 17132984]

Masliah E, Mallory M, Hansen L, DeTeresa R, Alford M, Terry R. Synaptic and neuritic alterations during the progression of Alzheimer's disease. Neurosci Lett. 1994; 174:67–72. [PubMed: 7970158]

Mazza M, Marano G, Traversi G, Bria P, Mazza S. Primary cerebral blood flow deficiency and Alzheimer's disease: shadows and lights. J Alzheimers Dis. 2011; 23:375–389. [PubMed: 21098977]

Melchor JP, Pawlak R, Strickland S. The tissue plasminogen activator-plasminogen proteolytic cascade accelerates amyloid-beta (Abeta) degradation and inhibits Abeta-induced neurodegeneration. J Neurosci. 2003; 23:8867–8871. [PubMed: 14523088]

Mosesson MW. Fibrinogen and fibrin structure and functions. J Thromb Haemost. 2005; 3:1894–1904. [PubMed: 16102057]

Nixon RA, Wegiel J, Kumar A, Yu WH, Peterhoff C, Cataldo A, Cuervo AM. Extensive involvement of autophagy in Alzheimer disease: an immuno-electron microscopy study. J Neuropathol Exp Neurol. 2005; 64:113–122. [PubMed: 15751225]

O'Mara S. The subiculum: what it does, what it might do, and what neuroanatomy has yet to tell us. J Anat. 2005; 207:271–282. [PubMed: 16185252]

Oakley H, Cole SL, Logan S, Maus E, Shao P, Craft J, Guillozet-Bongaarts A, Ohno M, Disterhoft J, Van Eldik L, et al. Intraneuronal beta-amyloid aggregates, neurodegeneration, and neuron loss in transgenic mice with five familial Alzheimer's disease mutations: potential factors in amyloid plaque formation. J Neurosci. 2006; 26:10129–10140. [PubMed: 17021169]

Paul J, Strickland S, Melchor JP. Fibrin deposition accelerates neurovascular damage and neuroinflammation in mouse models of Alzheimer's disease. J Exp Med. 2007; 204:1999–2008. [PubMed: 17664291]

Perez-Gracia E, Torrejon-Escribano B, Ferrer I. Dystrophic neurites of senile plaques in Alzheimer's disease are deficient in cytochrome c oxidase. Acta Neuropathol. 2008; 116:261–268. [PubMed: 18629521]

Prince, M.; Jackson, J. World Alzheimer Report 2009. Alzheimer's Disease International; 2009.

Ryu JK, McLarnon JG. A leaky blood-brain barrier, fibrinogen infiltration and microglial reactivity in inflamed Alzheimer's disease brain. J Cell Mol Med. 2009; 13:2911–2925. [PubMed: 18657226]

Schindler J, Jung S, Niedner-Schatteburg G, Friauf E, Nothwang HG. Enrichment of integral membrane proteins from small amounts of brain tissue. J Neural Transm. 2006; 113:995–1013. [PubMed: 16835696]

Selkoe, DJ. Cold Spring Harbor Perspectives in Biology. 2011. Alzheimer's Disease; p. 3

Solito E, Sastre M. Microglia function in Alzheimer's disease. Front Pharmacol. 2012; 3:14. [PubMed: 22363284]

Suh TT, Holmback K, Jensen NJ, Daugherty CC, Small K, Simon DI, Potter S, Degen JL. Resolution of spontaneous bleeding events but failure of pregnancy in fibrinogen-deficient mice. Genes Dev. 1995; 9:2020–2033. [PubMed: 7649481]

Tabrizi P, Wang L, Seeds N, McComb JG, Yamada S, Griffin JH, Carmeliet P, Weiss MH, Zlokovic BV. Tissue plasminogen activator (tPA) deficiency exacerbates cerebrovascular fibrin deposition and brain injury in a murine stroke model: studies in tPA-deficient mice and wild-type mice on a matched genetic background. Arterioscler Thromb Vasc Biol. 1999; 19:2801–2806. [PubMed: 10559029]

Terry RD, Masliah E, Salmon DP, Butters N, DeTeresa R, Hill R, Hansen LA, Katzman R. Physical basis of cognitive alterations in Alzheimer's disease: synapse loss is the major correlate of cognitive impairment. Ann Neurol. 1991; 30:572–580. [PubMed: 1789684]

Thambisetty M, Simmons A, Hye A, Campbell J, Westman E, Zhang Y, Wahlund LO, Kinsey A, Causevic M, Killick R, et al. Plasma biomarkers of brain atrophy in Alzheimer's disease. PloS one. 2011; 6:e28527. [PubMed: 22205954]

Vafadar-Isfahani B, Ball G, Coveney C, Lemetre C, Boocock D, Minthon L, Hansson O, Miles AK, Janciauskiene SM, Warden D, et al. Identification of SPARC-like 1 protein as part of a biomarker panel for Alzheimer's disease in cerebrospinal fluid. J Alzheimers Dis. 2012; 28:625–636. [PubMed: 22045497]

van Oijen M, Witteman JC, Hofman A, Koudstaal PJ, Breteler MM. Fibrinogen is associated with an increased risk of Alzheimer disease and vascular dementia. Stroke. 2005; 36:2637–2641. [PubMed: 16269641]

Viggars AP, Wharton SB, Simpson JE, Matthews FE, Brayne C, Savva GM, Garwood C, Drew D, Shaw PJ, Ince PG. Alterations in the blood brain barrier in ageing cerebral cortex in relationship to Alzheimer-type pathology: a study in the MRC-CFAS population neuropathology cohort. Neurosci Lett. 2011; 505:25–30. [PubMed: 21970975]

Weisel JW. Fibrinogen and fibrin. Adv Protein Chem. 2005; 70:247–299. [PubMed: 15837518]

Wirths O, Bayer TA. Neuron loss in transgenic mouse models of Alzheimer's disease. Int J Alzheimers Dis. 2010; 2010

Xu G, Zhang H, Zhang S, Fan X, Liu X. Plasma fibrinogen is associated with cognitive decline and risk for dementia in patients with mild cognitive impairment. Int J Clin Pract. 2008; 62:1070–1075. [PubMed: 17916180]

Yang H, Lyutvinskiy Y, Herukka SK, Soininen H, Rutishauser D, Zubarev RA. Prognostic polypeptide blood plasma biomarkers of Alzheimer's disease progression. J Alzheimers Dis. 2014; 40:659–666. [PubMed: 24503613]

Zamolodchikov D, Strickland S. Abeta delays fibrin clot lysis by altering fibrin structure and attenuating plasminogen binding to fibrin. Blood. 2012; 119:3342–3351. [PubMed: 22238323]

Zilkova M, Koson P, Zilka N. The hunt for dying neurons: insight into the neuronal loss in Alzheimer's disease. Bratisl Lek Listy. 2006; 107:366–373. [PubMed: 17262989]

Highlights for Review

- Fibrin deposition increases in the Alzheimer's disease brain and correlates with the degree of pathology.
- Fibrin(ogen) is present in areas of dystrophic neurites in the Alzheimer's disease brain.
- A decrease in fibrinogen levels improves neuronal health and ameliorates amyloid pathology in mouse models of Alzheimer's disease.

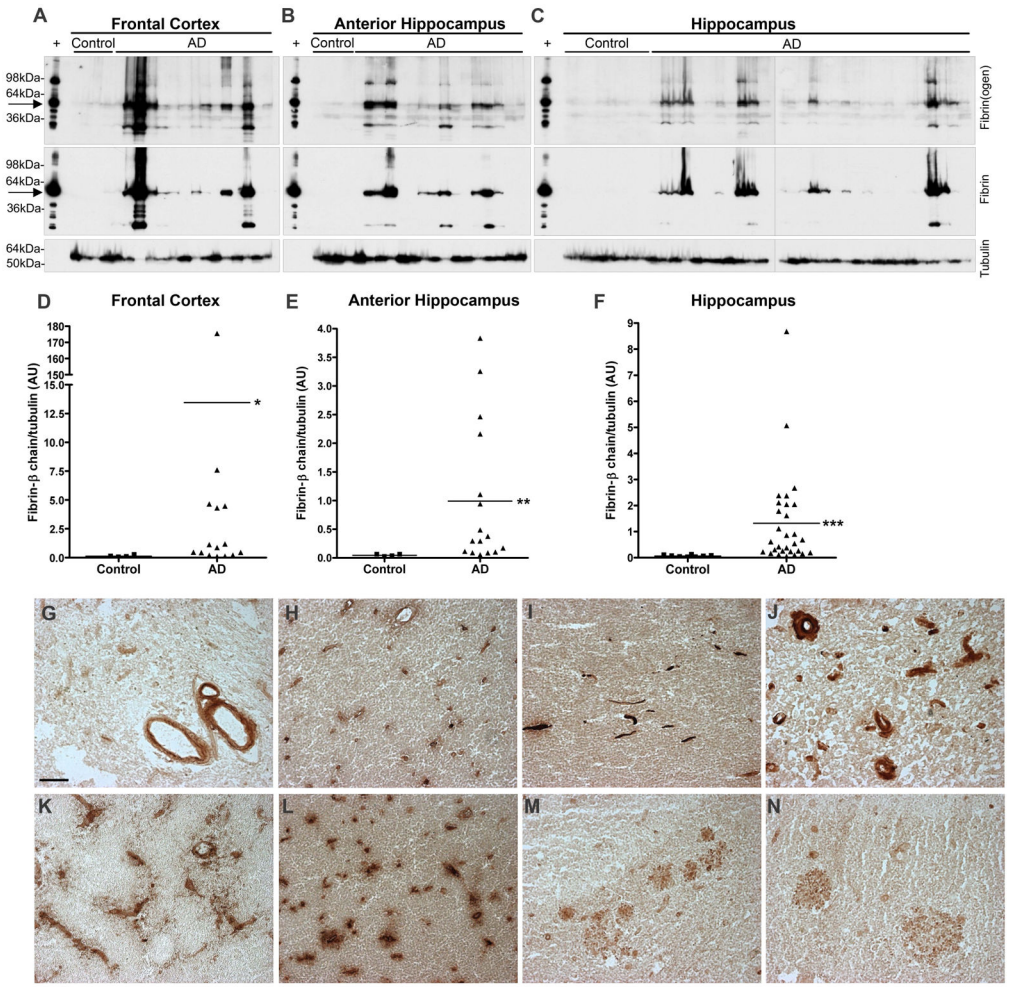

Figure 1. Fibrin deposition is increased in the human AD brain

Fibrin was isolated from the superior frontal cortex (A and D; n=4 control and 15 AD), the anterior hippocampus with entorhinal cortex (B and E; n=4 control and 16 AD), and the hippocampal formation with parahippocampal gyrus (C and F; n=8 control and 29 AD) of post-mortem samples from AD patients and non-demented controls. The insoluble fibrin-containing fraction was extracted and analyzed by Western blot. Fibrin was detected with an anti-fibrin(ogen) polyclonal antibody (top panels) or an anti-fibrin monoclonal antibody (59D8 (Hui et al., 1983); middle panels). Blots were re-probed with anti-tubulin antibody as loading control (bottom panels). Soluble fibrinogen is not present in these samples since it was removed during the extraction process. Each lane corresponds to an individual patient. Samples were run 4 different times, quantified, averaged, and plotted. Fibrin-β-chain (~52 kDa, arrows) was significantly increased in AD brains compared to non-demented controls in all regions analyzed (D–F). An *in vitro* fibrin clot prepared with human fibrinogen was run as positive control (+). Hippocampal samples were run on different gels due to space limitations (separated by a vertical line in C), and 4–6 samples were run on both gels to ensure results were similar between gels. Graphs show mean and Mann-Whitney test *$p<0.05$, **$p<0.01$ and ***$p<0.001$ comparing AD *vs* control. Fibrin immunohistochemistry was performed on human AD hippocampal cryosections using the 59D8 antibody and the

same set of patients used in (C). Fibrin was found intravascularly, lining big vessels (G) and/or blocking small ones (H–J), as well as extravascularly, in the vicinity of blood vessels (K and L) or forming plaque-like structures (M and N). Each image corresponds to a different human AD patient. Scale bar, 50 μm.

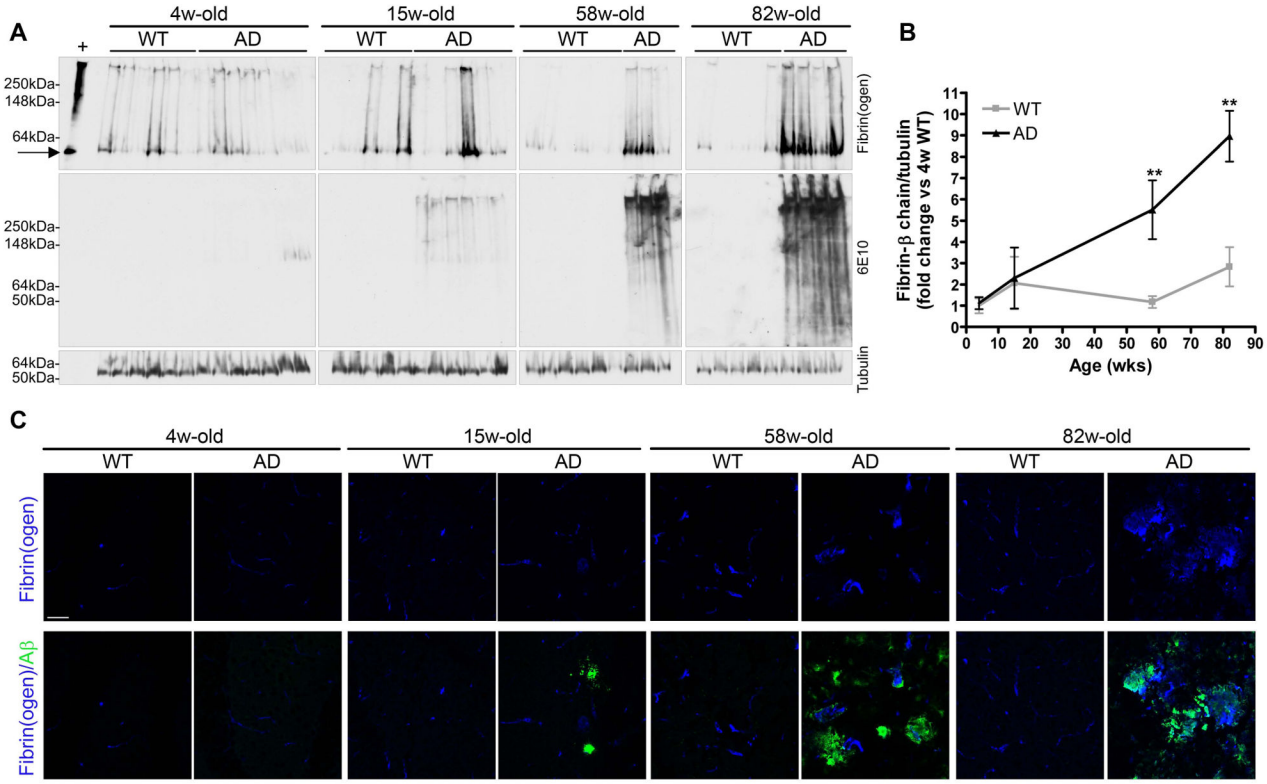

Figure 2. Fibrin deposition is increased in the brains of AD mice and correlates with Aβ pathology

(A) To detect fibrin deposited in the mouse brain, we used cortical and hippocampal samples from 4-, 15-, 58- and 82-week-old TgCRND8 mice (AD) and their wild type (WT) littermate controls (n=3–7/group). The insoluble (fibrin-containing) fraction was extracted, analyzed by Western blot, and probed with antibodies specific for murine fibrin(ogen) (top panels). Fibrinogen immunoreactivity was not detected because soluble fibrinogen was removed during the extraction protocol. The blots were re-probed with 6E10 antibody to detect Aβ pathology (middle panels) and with anti-tubulin antibody as loading control (bottom panels). Each lane corresponds to an individual mouse. Samples were run 5 times, quantified, averaged, and plotted by age and genotype. (B) Quantification indicates that the amount of fibrin-β-chain (~52 kDa, arrow in A) is significantly increased in the brains of 58- and 82-week-old AD mice compared to their littermate controls. This increase in fibrin deposition correlates with Aβ pathology. An *in vitro* fibrin clot prepared with mouse fibrinogen was used as positive control (+). Graph shows mean ± SEM and Student t-test **$p<0.01$ comparing AD *vs* WT. Two-way ANOVA and Bonferroni post-test analysis also showed the effect of genotype ($p=0.0003$) and age ($p=0.0001$) are significant. (C) Double immunofluorescence was performed on the same set of TgCRND8 mice and WT littermates used in (A). Representative confocal images from the cortex and hippocampus show that fibrin(ogen) (blue) and Aβ (green) staining increase with age and co-localize in the AD mouse brain. Scale bar, 40 μm.

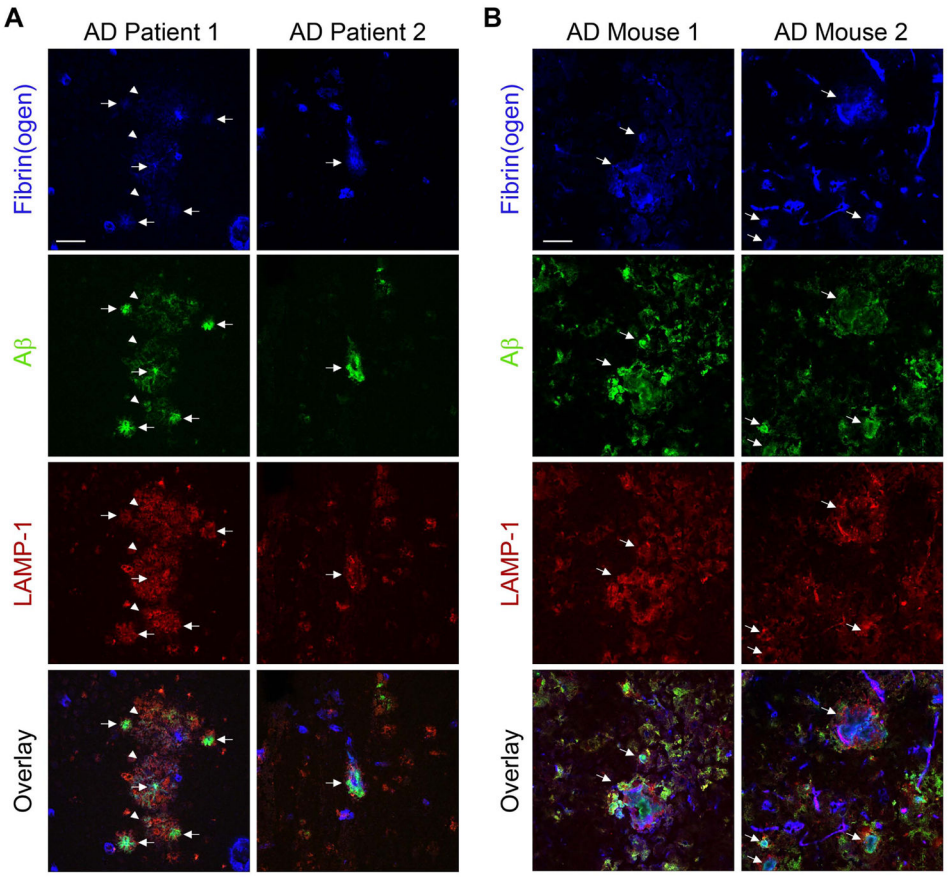

Figure 3. Fibrin(ogen) extravasation is present in areas of synaptic dysfunction in the human and mouse AD brain

(A) Postmortem hippocampal sections from AD patients were stained with an anti-fibrin(ogen) antibody (blue) in combination with anti-Aβ (green) and anti-LAMP-1 (red) antibodies to detect amyloid pathology and dystrophic neurites, respectively. Several patterns of fibrin(ogen) staining were found in the different human AD cases. Fibrin(ogen) co-localized with LAMP-1 in the core of amyloid plaques (arrows in AD Patient 1) but also with diffuse Aβ (arrowheads in AD Patient 2). Fibrin(ogen) was also found in areas of synaptic dysfunction and amyloid pathology close to blood vessels (arrow in AD Patient 2). Images correspond to two different human AD patients. Scale bar, 40 μm. (B) Immunofluorescent analysis of fibrin(ogen) (blue) in combination with dystrophic neurites (LAMP-1, red) and Aβ pathology (6E10, green) was performed on brain samples from 82-week-old TgCRND8 AD mice. A similar pattern throughout the brain was found in the AD mice with strong fibrin(ogen) staining in LAMP-1- and Aβ-positive areas (arrows). Representative images of the staining from two different 82-week-old TgCRND8 mice are shown. Scale bar, 40 μm.

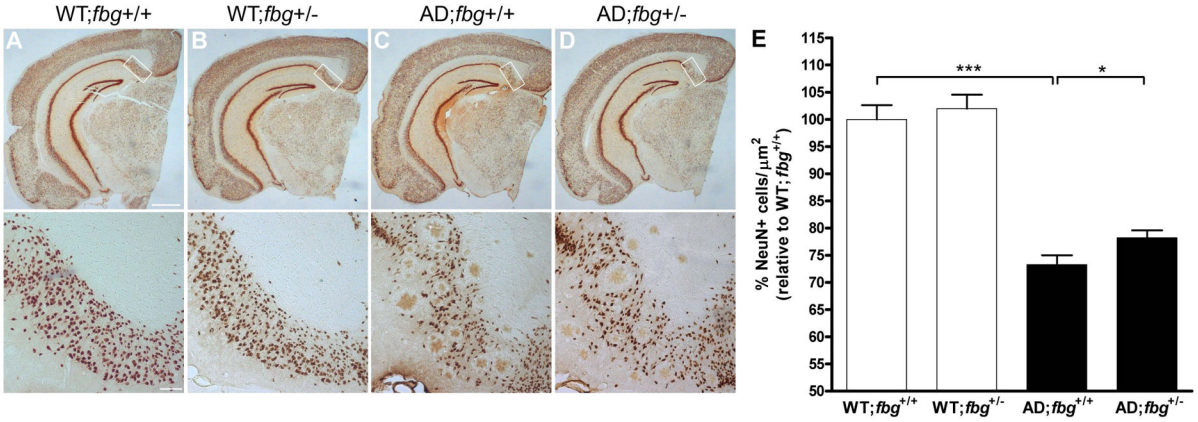

Figure 4. Decreasing fibrinogen levels ameliorates neuronal death in AD mice

Neuronal death was analyzed in TgCRND8 mice (AD; $fbg^{+/+}$), TgCRND8 mice heterozygous for a mutation in the *fibrinogen Aα chain* gene (AD; $fbg^{+/-}$), and their corresponding wild type littermates (WT; $fbg^{+/+}$ and WT; $fbg^{+/-}$). NeuN immunohistochemical analysis was performed to determine the number of neurons (A–D). The total number of NeuN-positive cells in the subiculum (boxed area, higher magnification in bottom panels) was quantified as explained in Methods. (E) Graph represents the percentage of neurons per μm^2 analyzed relative to WT; $fbg^{+/+}$ mice. AD; $fbg^{+/+}$ mice have significantly more neuronal death in the subiculum compared to WT controls, while AD; $fbg^{+/-}$ mice have significantly less neuronal death in this area of the brain compared to AD; $fbg^{+/+}$ mice. (n= 3–7 mice/group, ~ 8 sections/mouse). Average Bregma analyzed was kept at −3.0 mm per group and per mouse. Graph shows mean ± SEM and Student t-test ***$p<0.001$; *$p<0.05$. Scale bars, 500 μm (top panels) and 50 μm (bottom panels).

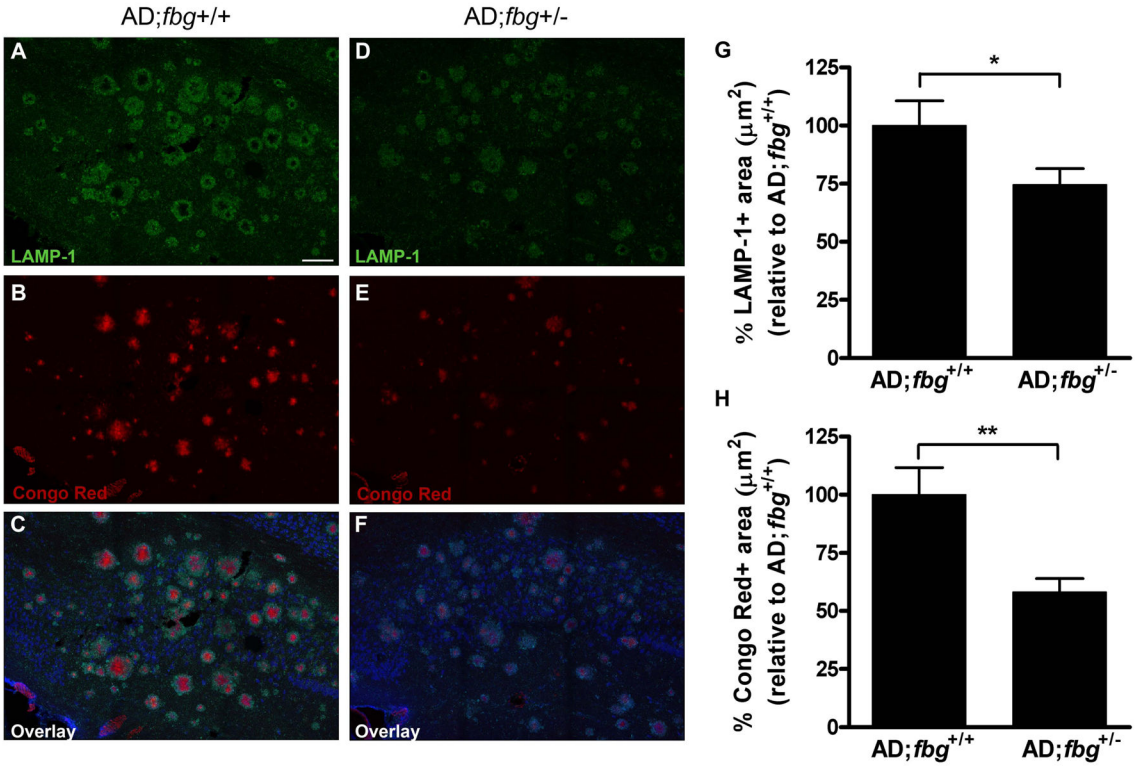

Figure 5. Decreasing fibrinogen levels reduces synaptic dysfunction and amyloid pathology in AD mice

Triple staining was performed on sections from TgCRND8 AD mice (AD; $fbg^{+/+}$) and AD mice heterozygous for a mutation in the *fibrinogen Aα chain* gene (AD; $fbg^{+/-}$). Anti-LAMP-1 antibody (A and D, green) and Congo Red staining (B and E, red) were used to identify dystrophic neurites and amyloid pathology, respectively. Sections were also analyzed with anti-NeuN antibody to observe neuronal bodies and identify the area of the subiculum (C and F, blue). Confocal Z-stacks of the subicular area were taken in all three channels, keeping constant conditions between groups. Each individual plane was quantified using NIH Image J software. Representative maximum projection tile-scan images are shown. Graphs represent the percentage of LAMP-1- (G) or Congo Red- (H) positive area *vs* the total subicular area analyzed, relative to the AD group. AD; $fbg^{+/-}$ mice presented a significant reduction in the amount of synaptic dysfunction as well as amyloid pathology in the subiculum (n= 2–4 mice/group, 2–3 sections/mouse). Graph shows mean ± SEM and Student t-test **p<0.01; *p<0.05. Scale bar, 100 μm.